Rom J Morphol Embryol 2022, 63(1):83–97 ISSN (print) 1220–0522, ISSN (online) 2066–8279 doi: 10.47162/RJME.63.1.08

ORIGINAL PAPER

RJME Romanian Journal of Morphology & Embryology http://www.rjme.ro/

Maternal alloxan exposure induces damage in rat offspring lumbar vertebrae and protective role of arachidonic acid

AYMAN SALAHELDEEN AMER, REFAAT SHEHATA MOHAMED, ASHRAF EDWARD BASTWROUS, MARTHA EMIL ADLY

Department of Human Anatomy and Embryology, Faculty of Medicine, Assiut University, Assiut, Egypt

Abstract

Background: Vertebral abnormalities in offspring of diabetic mothers make major challenges worldwide and were not sufficiently studied before. *Aim*: To investigate the effects of alloxan-induced diabetes on rats' lumbar vertebrae, and to assess the potential beneficial impact of arachidonic acid. *Materials and Methods*: Pregnant rats were randomly equally divided into four groups: control, alloxan-induced diabetes received alloxan injection 150 mg/kg, alloxan + arachidonic acid group received arachidonic acid 10 µg/animal then given alloxan injection, and arachidonic acid group received it, until offspring age of three weeks. Six male offspring from each group were included in this study at ages of newborn, three-week-old, two-month-old, and their body measurements were recorded. Lumbar vertebrae and pancreas specimens were examined by light microscopy, morphometry, transmission electron microscopy (TEM), and immunohistochemistry for insulin expression. *Results*: In alloxan-induced diabetes newborn, three-week-old, and two-month-old rats, body measurements were significantly declined, histomorphometry of 6th lumbar vertebrae revealed disorganized chondrocytes, with vacuolated cytoplasm, empty lacunae, diminished matrix staining, with areas devoid of cells. TEM showed shrunken reserve and proliferative cells, with irregular nuclei, and damaged mitochondria. In contrast, alloxan + arachidonic acid group had cytoarchitecture of lumbar vertebrae that were like control group. Histomorphometry of pancreas in alloxan-induced diabetes group showed significant reduction in pancreatic islets number and surface area, damaged pancreatic islet cells appeared atrophied with apoptotic nuclei, and very weak insulin immunostaining. Whereas alloxan + arachidonic acid group displayed healthy features of pancreatic islets, which resembled control group, with strong insulin immunostaining. *Conclusions*: Arachidonic acid mitigated alloxan-induced diabetes by its antidiabetic activity.

Keywords: diabetes mellitus, vertebral growth plate, chondrocytes ultrastructure, alloxan, arachidonic acid, immunohistochemistry.

Introduction

The prevalence of diabetes mellitus in pregnancy is high and continues to rise worldwide [1]. Diabetes mellitus is a chronic disease that incorporates various disorders and is characterized by a relative or absolute lack of insulin, resulting in hyperglycemia. Exposure of the fetus to hyperglycemia in pregnancy can cause long lasting problems in the offspring [2]. It was found that 30% of youth with type 2 diabetes were exposed to maternal diabetes *in utero* [3]. Despite increased clinical efforts to improve glycemic control during diabetic pregnancy, the rate of congenital malformations remains increased in studies of diabetic gestation of type 1 and type 2 diabetes [2, 4, 5].

The accumulated body of evidence denotes that diabetes during pregnancy leads to defective fetal growth [6]. Infants born to diabetic mother are shown to have hypocalcemia and lower bone mineral content at birth. In addition, hypoplasia of neurocranial, viscerocranial, forelimb, and hind limb bones have been observed in the fetuses of diabetic pregnant rats [7, 8]. The bones of the vertebral column are developed by the endochondral ossification where longitudinal bone growth is achieved. The endochondral ossification is a process occurring at the growth plate whereby a cartilaginous template is made and then replaced by bone [9, 10]. As the bone lengthening is taking place across the epiphyseal growth plate, damage to the plate prevents further growth. The endochondral bone growth activity is affected by several environmental factors, such as nutrition, medical treatments, and metabolic disorders [9, 11].

Alloxan is an agent which is used to induce a diabetes-like state in animals, is taken up by β-cells, and increases the production of reactive oxygen species (ROS) that lead to β-cell necrosis [12]. Alloxan-induced type 1 diabetes mellitus can be prevented by various polyunsaturated fatty acids (PUFAs). Of all the PUFAs tested, it was noted that arachidonic acid has the upper hand in defeating several health problems and may be beneficial in ameliorating the alloxan-induced cytotoxicity in rats [13, 14]. In cell culture, arachidonic acid was reported to be important for the functions of the cultured pancreatic β-cells [15]. Linkages between glucose metabolism and bone metabolism were suggested [16], and earlier research stated that the infants of diabetic mothers may have low arachidonic acid levels and develop insulin resistance in adulthood [6]. To the best of our knowledge, there is scarcity of previous research showing the effect of maternal diabetes on the vertebral epiphyseal plate formation and development. The effect of arachidonic acid on the development of vertebral epiphyseal plate in alloxan-induced diabetics was not studied before. The actual mechanism of action for arachidonic acid is still not fully clarified in literature [17]. Also, it is still not clear whether arachidonic acid can prevent any bony damage that may occur in diabetes. The lack of scientific articles

in the literature exploring the potential protective effects of arachidonic acid on alloxan-induced diabetic vertebral damage motivates the need to investigate this issue.

Aim

In this study, we will investigate the effect of alloxan-induced diabetes on the architecture and ultrastructure of the rat lumbar vertebra. The aim of this work was to fill the gap of knowledge on the efficacy of arachidonic acid to ameliorate the alloxan-induced diabetic damage of lumbar vertebra. In addition, this research tries to assess a possible explanation of the modulatory mechanism through which arachidonic acid may exert its antidiabetic protective effect.

Materials and Methods

Treatments

Alloxan monohydrate powder was obtained from Sigma-Aldrich, Inc., St Louis, Missouri, USA. Arachidonic acid was obtained from Santa Cruz Biotechnology, Inc., Dallas, TX, USA.

Experimental design and animals

A total of 24 adult female (three-month-old, weighing 200–250 g), and 12 adult male (three-month-old, weighing 200–250 g) albino rats were obtained from the Animal House, Faculty of Medicine, Assiut University, Assiut, Egypt. Rats were kept in metal cages under controlled room temperature, with 12 hours light/dark cycle during the research period. Food (standard rat chow) and water were available *ad libitum*. This experimental study was fully approved by the Local Ethical Committee and by the Institutional Review Board of the Faculty of Medicine, Assiut University (Approval No. 17200437) and was carried out in accordance with relevant guidelines and regulations. The experimental procedures affirm that all appropriate measures were taken to minimize animal pain or discomfort. This research was done in compliance with the Animal Research: Reporting of *In Vivo* Experiments (ARRIVE) guidelines and regulations (https://arriveguidelines.org). Female rats were mated with males overnight, and the presence of a vaginal plug that contains sperm was recorded as gestational day zero. Twenty-four pregnant rats were singly housed, and randomly and equally divided into four groups. Control group was given no treatment. Alloxan-induced diabetes group was given a single intraperitoneal injection of alloxan monohydrate, dissolved in 0.9% normal saline solution, given at a dose of 150 mg/kg body weight to induce diabetes mellitus [18]. Presence of diabetes was assessed by recording the rats' blood glucose level 72 hours and one week after injection of alloxan. Blood glucose was measured using On Call Plus® blood glucose monitor. Rats with blood glucose levels above 200 mg/dL were selected for this study group [18]. Mating was allowed one week after injection of alloxan. Alloxan + arachidonic acid group were given arachidonic acid orally daily for one week at dose of 10 µg/animal, followed by single intraperitoneal injection of alloxan monohydrate. Mating was allowed one week after injection of alloxan, and thereafter arachidonic acid was given once a week throughout the pregnancy and until the end of lactation (offspring age of three weeks) [14]. Arachidonic acid group were given arachidonic acid orally daily for one week at dose of 10 µg/animal, and then once a week until the offspring age of three weeks [14]. The research period continued until the offspring age of two months.

Six male offspring from each group were included in this study at the ages of newborn, three-week-old, and two-month-old. Rats were anaesthetized by Ether inhalation and subjected to intracardiac perfusion of 0.9% normal saline into the left ventricle, then euthanized by cervical dislocation for tissue specimen collection. The crown-rump, snout-rump, crown-heel lengths, and the body weight were measured for statistical analysis.

Histomorphometric study

At each of the previous ages, the lumbar vertebrae were extracted, fixed in 10% Formalin solution for 24–72 hours for light microscopy, or in 2.5% Glutaraldehyde for transmission electron microscopy (TEM). The specimens of the three-week-old and two-month-old rats were decalcified by adding 35 mL Formic acid in 65 mL 20% Sodium citrate and kept for 10 days. Bone specimens were prepared for paraffin embedding, sectioned at 8–10 µm, then stained with Hematoxylin–Eosin (HE) to display the general histological structure, and Masson's trichrome technique to demonstrate the collagen fibers. Semithin sections (1 µm) stained with Toluidine blue were also prepared for light microscopy to demonstrate glycosaminoglycan content of the cartilage matrix. Ultra-thin sections (450–500 Å) stained using Uranyl acetate and Lead citrate were prepared from the epiphyseal growth plate of 6th lumbar vertebrae to assess the chondrocytes, reserve cells and proliferative cells, for TEM study. The stained ultrathin sections were examined by Jeol-JEM-100 CX-II electron microscope (JEOL, Tokyo, Japan) and images were captured at the Electron Microscopy Unit of Assiut University, Egypt. Immunohistochemical (IHC) staining was performed following a previously published protocol [19] to evaluate the immunoexpression of insulin in the pancreatic islets using anti-insulin primary antibodies (obtained from ABclonal Company, Woburn, MA, USA, 1:500 dilution) for all groups to verify the islet structure and to assess the potential antidiabetic effect of arachidonic acid. For the IHC detection of insulin, Avidin–Biotin–Peroxidase technique was used [19]. Insulin-positive immunostained cells showed brown cytoplasmic staining.

All stained slides were examined with an Olympus CX41 microscope, and photos were taken by an Olympus DP72 charge-coupled device (CCD) digital camera (Olympus Corporation, Tokyo, Japan) attached to the microscope. HE-stained sections of the lumbar vertebrae and pancreatic islets were morphometrically analyzed by using an image analysis system (Olympus cellSens Standard 1.16 software, Olympus Corporation, Tokyo, Japan) at the Department of Human Anatomy and Embryology, Faculty of Medicine, Assiut University. The thickness of the epiphyseal growth plate of lumbar vertebrae, number of pancreatic islets, surface area of the islets, and number of β-cells were recorded.

Statistical analysis

GraphPad Prism Software version 5 (GraphPad Software, Inc., La Jolla, CA, USA) was used for data analysis. Data were presented as mean ± standard deviation (SD). Comparison among groups was carried out using one-way analysis of variance (ANOVA) followed by Bonferroni's

post hoc test. Differences of $p<0.05$ were statistically significant.

Results

Effects of arachidonic acid on the gross morphological measurements of alloxan-induced diabetes newborn rats

Gross morphological measurements were conducted including the body weight, crown rump length, snout rump length, crown heel length and thickness of the epiphyseal growth plate of the 6th lumbar vertebrae of the newborn rats. Alloxan-induced diabetes group showed significant reductions in all parameters as compared to the control group (Table 1). The results of the alloxan + arachidonic acid group showed nonsignificant difference when compared to the control group, while there was significant difference when compared to the alloxan-induced diabetes group (Table 1). In arachidonic acid group, the results showed nonsignificant difference as compared to the control group, while there was significant difference when compared to the alloxan-induced diabetes group (Table 1).

Table 1 – ***Effect of arachidonic acid on the body and vertebral measurements of newborn rats suffering from alloxan-induced diabetes***

Group	Control	Alloxan-induced diabetes	Alloxan + arachidonic acid	Arachidonic acid	*p*-value
Weight [g]	6.80±0.48[a]	4.57±0.42[b]	6.72±0.33[a]	6.88±0.46[a]	<0.01
Crown rump length [cm]	4.95±0.19[a]	4.00±0.25[b]	5.00±0.14[a]	5.05±0.19[a]	<0.05
Snout rump length [cm]	4.32±0.12[a]	3.23±0.14[b]	4.30±0.13[a]	4.37±0.12[a]	<0.05
Crown heel length [cm]	5.37±0.12[a]	4.15±0.14[b]	5.18±0.15[a]	5.35±0.11[a]	<0.05
Epiphyseal growth plate thickness of 6th lumbar vertebra [μm]	263.23±8.24[a]	221.60±15.58[b]	261.40±11.31[a]	266.88±8.24[a]	<0.0001

Results were expressed as the mean ± SD of six rats per group. [a,b]Different letters indicated significant differences at $p<0.05$ (one-way ANOVA followed by Bonferroni's *post hoc* test). ANOVA: Analysis of variance; SD: Standard deviation.

Effects of arachidonic acid on the gross morphological measurements of alloxan-induced diabetes three-week-old rats

The morphological data analysis of the three-week-old rats indicated significant reductions in the body weight, crown rump length, snout rump length, crown heel length and thickness of the epiphyseal growth plate of the 6th lumbar vertebrae of alloxan-induced diabetes group as compared to the control group (Table 2). In alloxan + arachidonic acid group, the results showed nonsignificant difference as compared to the control group, while there was significant difference when compared to the alloxan-induced diabetes group (Table 2). Furthermore, the results of the arachidonic acid group revealed nonsignificant difference when compared to the control group, whereas there was significant difference when compared to the alloxan-induced diabetes group (Table 2).

Table 2 – ***Effect of arachidonic acid on the body and vertebral measurements of three-week-old rats suffering from alloxan-induced diabetes***

Group	Control	Alloxan-induced diabetes	Alloxan + arachidonic acid	Arachidonic acid	*p*-value
Weight [g]	31.17±3.92[a]	22.67±2.07[b]	31.83±4.26[a]	31.50±3.89[a]	<0.001
Crown rump length [cm]	9.03±0.33[a]	7.37±0.36[b]	8.93±0.37[a]	8.97±0.34[a]	<0.05
Snout rump length [cm]	8.87±0.30[a]	7.05±0.40[b]	8.75±0.37[a]	8.78±0.36[a]	<0.05
Crown heel length [cm]	11.07±0.40[a]	9.35±0.36[b]	10.92±0.29[a]	10.98±0.33[a]	<0.05
Epiphyseal growth plate thickness of 6th lumbar vertebra [μm]	374.21±9.31[a]	314.70±8.83[b]	367.81±12.00[a]	372.47±7.89[a]	<0.0001

Results were expressed as the mean ± SD of six rats per group. [a,b]Different letters indicated significant differences at $p<0.05$ (one-way ANOVA followed by Bonferroni's *post hoc* test). ANOVA: Analysis of variance; SD: Standard deviation.

Effects of arachidonic acid on the gross morphological measurements of alloxan-induced diabetes two-month-old rats

As shown in Table 3, the morphological data analysis of the two-month-old rats indicated significant reductions in the body weight, crown rump length, snout rump length, crown heel length and thickness of the epiphyseal growth plate of the 6th lumbar vertebrae of alloxan-induced diabetes group as compared to the control group. In the alloxan + arachidonic acid group, the results showed nonsignificant difference as compared to the control group, while there was significant difference when compared to the alloxan-induced diabetes group (Table 3).

Table 3 – ***Effect of arachidonic acid on the body and vertebral measurements of two-month-old rats suffering from alloxan-induced diabetes***

Group	Control	Alloxan-induced diabetes	Alloxan + arachidonic acid	Arachidonic acid	*p*-value
Weight [g]	150.00±2.28[a]	144.33±1.63[b]	149.50±3.39[a]	151.00±2.61[a]	<0.01
Crown rump length [cm]	14.17±0.68[a]	12.00±0.45[b]	14.00±0.95[a]	14.42±0.92[a]	<0.001
Snout rump length [cm]	13.17±0.68[a]	11.00±0.45[b]	13.00±0.95[a]	13.42±0.92[a]	<0.001
Crown heel length [cm]	18.00±0.89[a]	15.87±0.53[b]	17.92±0.86[a]	18.33±0.82[a]	<0.001
Epiphyseal growth plate thickness of 6th lumbar vertebra [μm]	385.66±3.08[a]	317.03±11.68[b]	384.67±3.43[a]	387.43±1.82[a]	<0.0001

Results were expressed as the mean ± SD of six rats per group. [a,b]Different letters indicated significant differences at $p<0.05$ (one-way ANOVA followed by Bonferroni's *post hoc* test). ANOVA: Analysis of variance; SD: Standard deviation.

Moreover, the results of the arachidonic acid group revealed nonsignificant difference when compared to the control, whereas there was significant difference when compared to the alloxan-induced diabetes group (Table 3).

Effects of arachidonic acid on the histopathological features of vertebrae of alloxan-induced diabetes newborn rats

The histological examination of the lumbar (L5 and L6) vertebrae in the control group showed normal features of vertebral body, which was formed of centrum and two peripheral epiphyseal growth plates of hyaline cartilage. The chondrocytes in the epiphyseal growth plates were arranged as follows (Figure 1, a and i):

(*i*) Zone of reserve cells: the cells in this zone were small, rounded or spindle shaped, seen both within and without lacuna.

(*ii*) Zone of proliferative cells: the cells in this zone were flattened and enclosed inside lacunae, with a characteristic columnar arrangement parallel to the growth axis.

(*iii*) Zone of hypertrophied cells: the hypertrophied chondrocytes were larger than the previous cells. They are enclosed inside large, rounded lacunae.

(*iv*) Calcification zone: the hypertrophied chondrocytes in this zone were degenerated leaving lacunae, which were invaded by bone cells from the marrow-filled spaces of the centrum.

The centrum of each vertebra showed a well-developed primary center of ossification with multiple spaces in the calcified cartilage representing empty confluent lacunae after chondrocytes degeneration (Figure 1a). The inter-vertebral disc appeared to be composed of an outer fibrous layer (*annulus fibrosus*) and a gelatinous core (*nucleus pulposus*) (Figure 1, a and e). To evaluate the distribution and arrangement of the collagen fibers, we employed Masson's trichrome technique. The control group showed normal homogenous distribution of collagen fibers (green color) in the matrix between the growing chondrocytes in the epiphyseal growth plates (Figure 1e). Semithin sections of the epiphyseal plates stained with Toluidine blue normal distribution of the staining in the cartilage matrix (Figure 1m). TEM examination of the reserve cell zone of the epiphyseal plate of the 6th lumbar vertebra showed oval cells with rounded or oval nucleus, rough endoplasmic reticulum (RER), lipid granules, many mitochondria, and multiple cytoplasmic processes. The reserve cells were surrounded by a narrow clear pericellular space. Outside this zone, a fine network of thin fibrils was seen in the extracellular matrix (ECM) (Figure 2, a and e). TEM examination of the proliferative cell zone of the epiphyseal plate of the 6th lumbar vertebra showed flattened cells located in pairs and enclosed in lacunae that were separated from each other by transverse septa (TS). The proliferative cells had multiple cytoplasmic processes with well-formed nucleus, RER, and visible lipid granules in the cytoplasm. The surrounding ECM was rich in collagen fibrils (Figure 2, i and m).

In alloxan-induced diabetes group, there was apparent decreased thickness of the epiphyseal growth plates and less developed primary ossification centers as compared to the control group. The growing chondrocytes appeared small, disorganized, and distorted, with vacuolated cytoplasm (Figure 1, b and j). In addition, empty lacunae, and areas of the matrix devoid of cells were observed. Using Masson's trichrome technique, the epiphyseal growth plates showed diminished staining of the matrix in between the growing chondrocytes (Figure 1f); and the semithin sections showed diminished staining of the cartilage matrix as compared to the controls (Figure 1n). TEM examination of the reserve cell zone of the epiphyseal plate of the 6th lumbar vertebra showed shrinkage of the cells with irregular outline, irregular nucleus, less developed RER, damaged mitochondria, and cytoplasmic vacuolations. These findings suggest apoptosis. The surrounding pericellular space appeared widened with less collagen fibrils in the ECM (Figure 2, b and f). TEM examination of the proliferative cell zone of the epiphyseal plate of the 6th lumbar vertebra showed irregular outline with irregular nucleus, cytoplasmic vacuolations and less developed RER. The cells were surrounded by widened lacunae with sparse collagen fibrils in the ECM (Figure 2, j and n).

In alloxan + arachidonic acid group, the cytoarchitecture of the lumbar vertebrae was returned to the normal. The chondrocytes in the epiphyseal growth plates were arranged in the same four zones as in the control group, with no visible cellular changes (Figure 1, c, g, k and o). TEM examination of the reserve cell zone of the epiphyseal plate of the 6th lumbar vertebra showed the cells appeared oval with well-formed nucleus, RER, lipid granules, many mitochondria, and multiple cytoplasmic processes (Figure 2, c and g). TEM examination of the proliferative cell zone of the epiphyseal plate of the 6th lumbar vertebra showed flattened cells, which lay in pairs and enclosed in lacunae that were separated from each other by TS (Figure 2, k and o). There were no marked changes in both zones as compared to the controls.

In arachidonic acid group, the chondrocytes in the epiphyseal growth plates were arranged in four zones similar to the control group with no evident histological changes (Figure 1, d, h, l and p). TEM examination of the reserve cell zone of the epiphyseal plate of the 6th lumbar vertebra showed the cells appeared as normal similar to the control group, with well-formed nucleus, rich cytoplasmic organelles, and multiple cytoplasmic processes (Figure 2, d and h). In addition, TEM examination of the proliferative cell zone of the epiphyseal plate of the 6th lumbar vertebra showed no changes as compared to the controls (Figure 2, l and p).

Effects of arachidonic acid on the histopathological features of vertebrae of alloxan-induced diabetes three-week-old rats

In the control group, the sagittal sections of the lumbar (L5 and L6) vertebrae showed increase in size of the vertebral body as compared to the newborns. The vertebrae appeared with centrum and two peripheral areas of epiphyseal growth plates where the chondrocytes were arranged in the same four zones as in the newborn rat (Figure 3, a and i). Using Masson's trichrome technique, the epiphyseal growth plates showed normal homogenous distribution of the green color in the matrix between the growing chondrocytes (Figure 3e). Semithin sections of the epiphyseal plate of the 6th lumbar vertebrae showed normal distribution of Toluidine blue staining in the cartilage matrix (Figure 3m). TEM examination of the reserve cell

zone of the epiphyseal plate of the 6th lumbar vertebra showed triangular-shaped cells surrounded by pericellular zone. The nuclei occupy a large part of the cells, with well-developed RER, mitochondria, and apparent cytoplasmic processes. The cells are surrounded by ECM rich in collagen fibrils (Figure 4, a and e).

In alloxan-induced diabetes group, there was apparent decreased thickness of the epiphyseal growth plates and less developed primary ossification centers as compared to the control group. Growing chondrocytes were small-sized, disorganized, and distorted, with vacuolated cytoplasm. The ECM showed empty lacunae, with areas devoid of cells suggestive of cellular disintegration, and diminished staining with Masson's trichrome and Toluidine blue (Figure 3, b, f, j, and n). By TEM, the reserve cell zone of the epiphyseal plate of the 6th lumbar vertebra showed shrunken cells with irregular outline, irregular-shaped nuclei, less developed RER, damaged mitochondria, and cytoplasmic vacuolations. The findings suggest chondrocyte apoptosis. The surrounding pericellular space appeared widened with less collagen fibrils in the ECM (Figure 4, b and f).

In alloxan + arachidonic acid group, the histological features of the lumbar vertebrae were returned to the normal, with no apparent cellular changes (Figure 3, c and k). There was normal homogenous distribution of collagen fibers as seen by using both Masson's trichrome and Toluidine blue stainings (Figure 3, g and o). TEM examination of the reserve cell zone of the epiphyseal plate of the 6th lumbar vertebra showed triangular cells, with oval nucleus, and cellular organelles like those of the control (Figure 4, c and g).

In arachidonic acid group, the histological findings of the lumbar vertebrae were similar to those of the control group (Figure 3, d, h, l and p). In addition, the ultrastructure of the reserve cell zone of the epiphyseal plate of the 6th lumbar vertebra showed features like those of the control group (Figure 4, d and h).

Effects of arachidonic acid on the histopathological features of vertebrae of alloxan-induced diabetes two-month-old rats

The sagittal sections of the lumbar (L5 and L6) vertebrae in the control group showed increase in size of the vertebral body as compared to the three-week-old rats. The vertebrae appeared with centrum and two peripheral areas of the epiphyseal growth plates where the chondrocytes were arranged in the same four zones as in the three-week-old rats (Figure 5, a and i). Using Masson's trichrome technique, the epiphyseal growth plates showed normal homogenous distribution of the green color in the matrix between the healthy growing chondrocytes (Figure 5e). Semithin sections of the epiphyseal plate of the 6th lumbar vertebrae showed normal distribution of Toluidine blue staining in the cartilage matrix (Figure 5m).

In alloxan-induced diabetes group, there was apparent decreased thickness of the epiphyseal growth plates and less developed primary ossification centers as compared to the control group. The growing chondrocytes were small-sized, disorganized, and having vacuolated cytoplasm. The ECM showed empty lacunae, with areas without cells indicative of cellular disintegration, and diminished staining with Masson's trichrome and Toluidine blue (Figure 5, b, f, j and n). In alloxan + arachidonic acid group, the histological features of the lumbar vertebrae were returned to the normal picture, with no apparent cellular changes (Figure 5, c and k). There was normal homogenous distribution of collagen fibers as seen by using both Masson's trichrome and Toluidine blue stainings (Figure 5, g and o). In arachidonic acid group, the histological findings of the lumbar vertebrae were similar to those of the control group (Figure 5, d, h, l and p).

Effects of arachidonic acid on the random blood glucose levels of rats' mothers suffering from alloxan-induced diabetes

Random blood glucose levels were recorded from the rats' mothers of all studied groups. In alloxan-induced diabetes group, the blood glucose level was significantly much higher than the control group (Table 4). There were nonsignificant differences between the alloxan + arachidonic acid group, and arachidonic acid group as compared to the control. On the other hand, there was significant difference between the alloxan + arachidonic acid group when compared to the alloxan-induced diabetes group. Also, there was a significant difference between the arachidonic acid group when compared to the alloxan-induced diabetes group (Table 4).

Table 4 – ***Effect of arachidonic acid on the blood glucose levels of the rats' mothers suffering from alloxan-induced diabetes***

Group	Control	Alloxan-induced diabetes	Alloxan + arachidonic acid	Arachidonic acid	*p*-value
Blood glucose level [mg/dL]	80.25±5.56[a]	311.75±82.79[b]	86.75±6.40[a]	78.50±6.25[a]	<0.0001

Results were expressed as the mean ± SD of six rats per group. [a,b]Different letters indicated significant differences at $p<0.05$ (one-way ANOVA followed by Bonferroni's *post hoc* test). ANOVA: Analysis of variance; SD: Standard deviation.

Effects of arachidonic acid on the histology, insulin immunohistochemistry, and morphometric indices of pancreatic islets in the rats' mothers suffering from alloxan-induced diabetes

The histology of the pancreas in the rats' mothers of the control group showed normal architecture of the pancreatic islets, which were seen interspersed between the pancreatic acini, with distinct border between exocrine (pancreatic acini) and endocrine portions (islets of Langerhans) (Figure 6, a and e). The islet cells appeared healthy with vesicular nuclei. Immunohistochemistry revealed intense brown staining of insulin immunoreactivity (Figure 6i) within the cytoplasm of the β-cells of the pancreatic islets. In alloxan-induced diabetes group, the pancreatic islets were small-sized as compared to the control group with less distinct border between exocrine and endocrine portions, and the islet cells appeared atrophied with apoptotic nuclei (Figure 6, b and f). Immunohistochemistry revealed very weak insulin immunostaining in the cytoplasm of pancreatic β-cells (Figure 6j). Histomorphometry analysis indicated highly significant reduction in the number of pancreatic islets and their surface area and decrease in number of β-cells per islet (Table 5; Figure 7). Whereas alloxan + arachidonic acid group showed healthy features of the pancreatic islets,

which resembled the control group (Figure 6, c and g), strong insulin immunoreactivity (Figure 6k), with normalized histomorphometry data (Table 5; Figure 7). In arachidonic acid group, the pancreatic islets appeared normal (Figure 5, d and h), with strong insulin immunostaining (Figure 6l), and normal morphometric parameters (Table 5; Figure 7).

Table 5 – ***Effect of arachidonic acid on pancreatic morphometric indices of the rats' mothers suffering from alloxan-induced diabetes***

Group	Control	Alloxan-induced diabetes	Alloxan + arachidonic acid	Arachidonic acid	*p*-value
No. of pancreatic islets (per area 8 785 913.29 μm^2)	5.00±0.89^a	1.50±0.55^b	4.83±0.75^a	5.17±0.98^a	<0.0001
Surface area of pancreatic islets (μm^2)	49 843.04±10 668.7^a	10917.40±1947.1^b	49 348.99±10 396.2^a	48 258.52±11 494.4^a	<0.0001
No. of *β*-cells per islet	108.8±9.5^a	24.3±7.5^b	106.0 ± 9.1^a	107.8±8.99^a	<0.0001

Results were expressed as the mean ± SD of six rats per group. ^{a,b}Different letters indicated significant differences at $p<0.05$ (one-way ANOVA followed by Bonferroni's *post hoc* test). ANOVA: Analysis of variance; SD: Standard deviation.

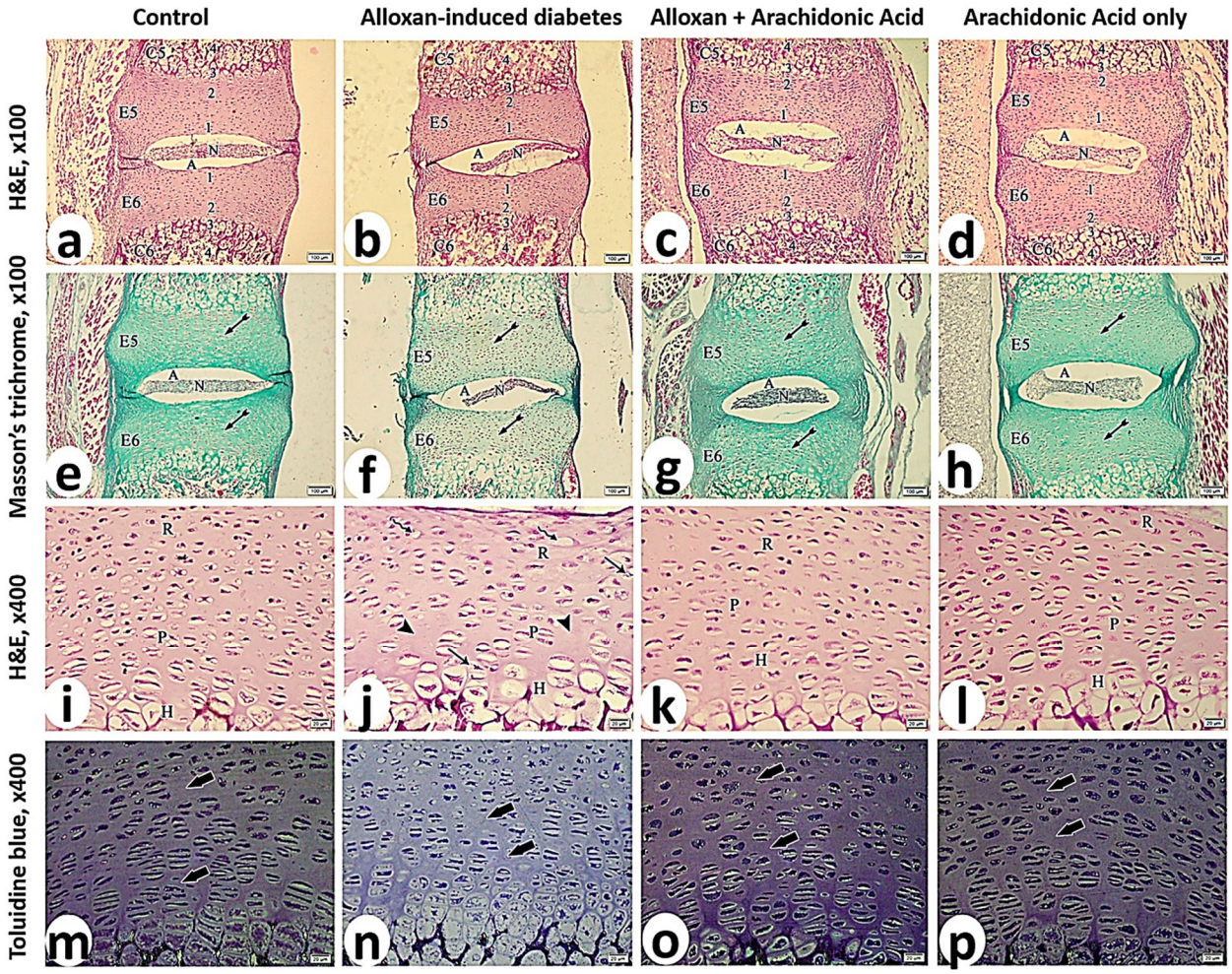

Figure 1 – ***Photomicrographs of sagittal sections in the newborn rats' 5th and 6th lumbar vertebrae showed the protective effect of arachidonic acid on alloxan-induced diabetes. Control group in (a, e, i and m) showed the normal histology of epiphyseal growth plates (E5 and E6) of the vertebrae, which had four zones of growing chondrocytes. The epiphyseal growth plates show normal homogenous distribution of green color (tailed arrow), and Toluidine blue staining in the cartilage matrix (thick arrow) between the growing chondrocytes. Alloxan-induced diabetes group in (b, f, j and n) showed apparent reduction in thickness of E5 and E6, with distortion and disorganization of small-sized chondrocytes with vacuolated cytoplasm (arrow). Diminished staining of the matrix (tailed arrow), empty lacunae (wavy arrow), areas of the matrix devoid of cells (arrowhead), and less developed primary ossification centers were seen. Alloxan + arachidonic acid in (c, g, k and o) showed healthy epiphyseal growth plates (E5 and E6) of the vertebrae, with four zones of growing chondrocytes, and well-developed primary ossification centers in centrum. Arachidonic acid group in (d, h, l and p) showed normal histology of epiphyseal growth plates (E5 and E6) of the vertebrae, with well-developed primary ossification centers. Note the intervertebral disk with nucleus pulposus (N) and annulus fibrosus (A). HE staining: (a–d and i–l) ×100, scale bar 100 μm. Masson's trichrome technique: (e–h) ×100, scale bar 100 μm. Toluidine blue staining: (m–p) ×400, scale bar 20 μm. 1: Reserve (R) cells; 2: Proliferative (P) cells; 3: Hypertrophied (H) cells; 4: Calcification (C) zone with well-developed primary ossification centers in centrum; HE: Hematoxylin–Eosin.***

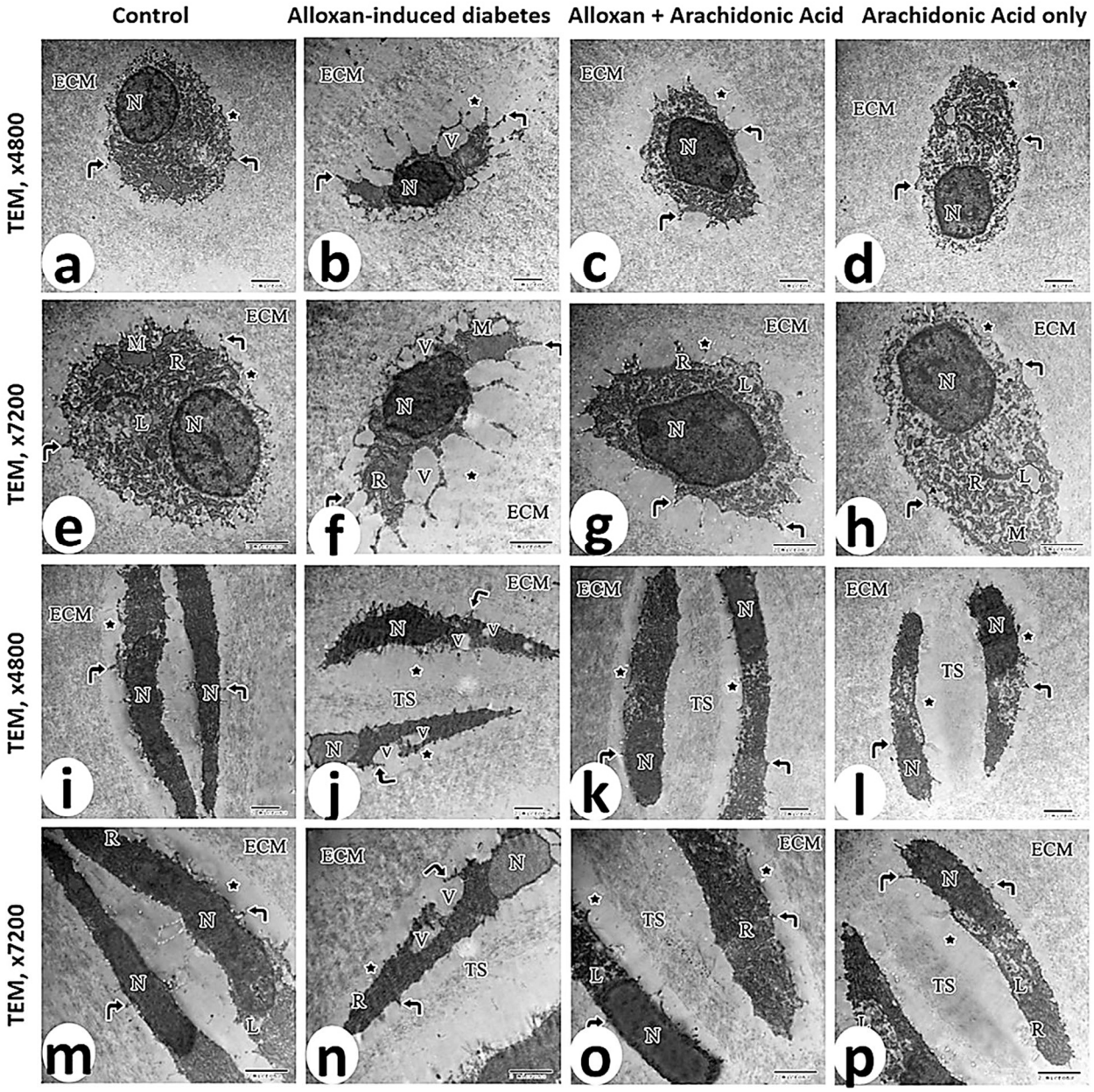

Figure 2 – ***Transmission electron micrographs of ultrathin sections in the newborn rats' 6th lumbar vertebrae showing the protective effect of arachidonic acid on alloxan-induced diabetes. Control group showed the normal ultrastructure of reserve zone cells (a and e) and proliferative zone cells (i and m) of the epiphyseal plates. The reserve cell had oval nucleus (N), rough endoplasmic reticulum (R), lipid granules (L), many mitochondria (M), multiple cytoplasmic processes (curved arrows), pericellular space (asterisk) and extracellular matrix (ECM) rich in collagen fibrils. The proliferative cells appear flattened and enclosed in lacunae (asterisk). The lacunae are separated from each other by transverse septa (TS). The cells show well-formed nucleus (N), multiple cytoplasmic processes (curved arrows), with surrounding ECM rich in collagen fibrils. Alloxan-induced diabetes group showed shrunken reserve cells (b and f) with irregular nucleus (N), cytoplasmic vacuolations (V), damaged mitochondria (M), typical of cell undergoing apoptosis, widened pericellular space (asterisk) and less collagen fibrils in the ECM. The proliferative cells (j and n) showed irregular outline with irregular nucleus (N), cytoplasmic vacuolations (V), widened lacunae (asterisk), and less developed rough endoplasmic reticulum (R). Alloxan + arachidonic acid group in (c, g, k and o) showed healthy appearance of the reserve and proliferative cells, which had oval nuclei (N), multiple cytoplasmic processes (curved arrows), many mitochondria (M), pericellular space (asterisk) and ECM rich in collagen fibrils. The proliferative cells were enclosed in lacunae (asterisk), which were separated from each other by TS. Arachidonic acid group in (d, h, l and p) showed the normal features of reserve and proliferative cells. Uranyl acetate and Lead citrate staining, transmission electron microscopy (TEM): (a–d and i–l) ×4800; (e–h and m–p) ×7200; scale bar 2 μm.***

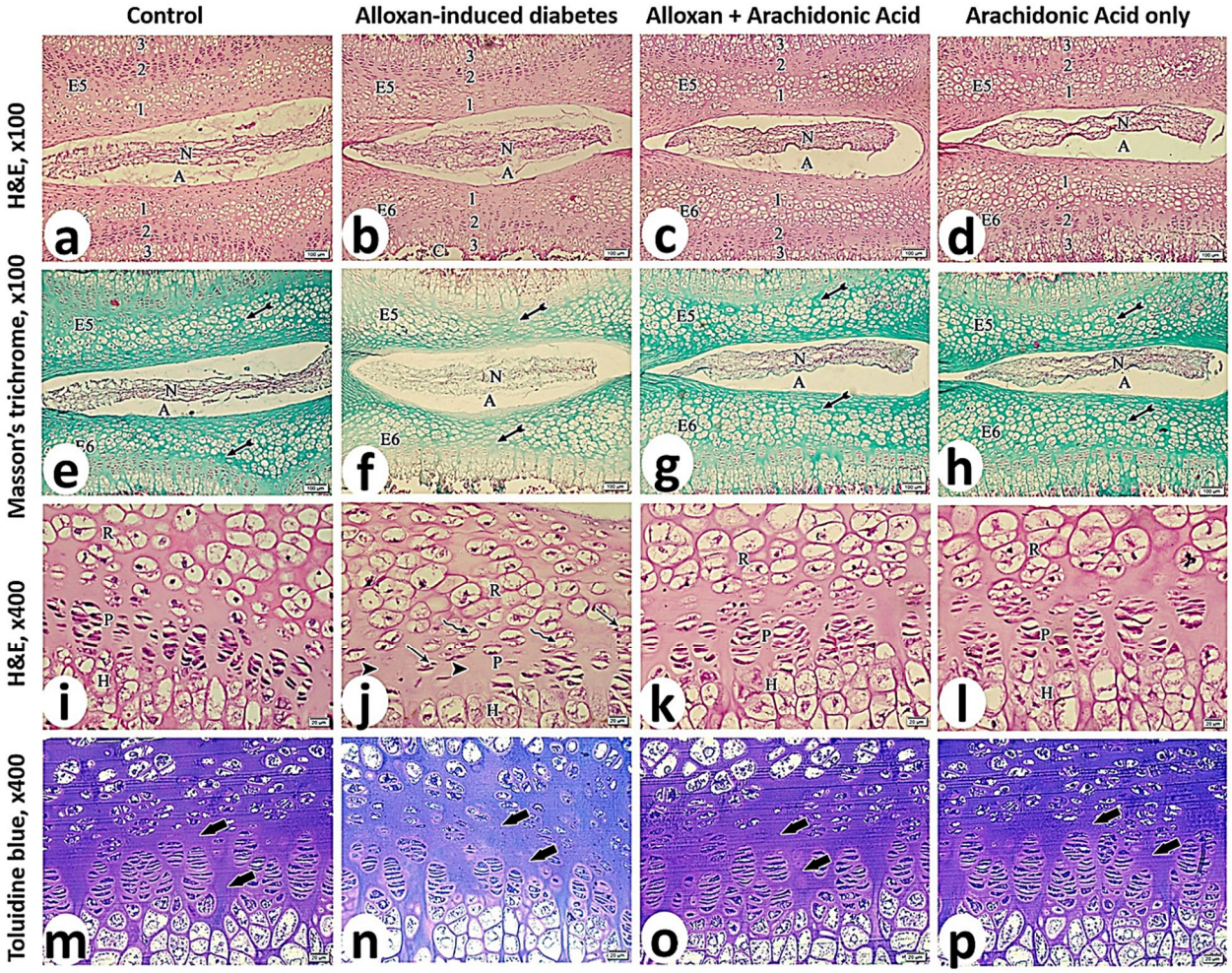

Figure 3 – ***Photomicrographs of sagittal sections in the three weeks old rats' 5th and 6th lumbar vertebrae showed the protective effect of arachidonic acid on alloxan-induced diabetes. Control group in (a, e, i and m) showed the epiphyseal growth plates (E5 and E6), with normal appearance of the vertebrae, which had zones of growing chondrocytes. The epiphyseal growth plates show normal homogenous distribution of green color (tailed arrow), and Toluidine blue staining in the cartilage matrix (thick arrow) between the growing chondrocytes. Alloxan-induced diabetes group in (b, f, j and n) showed reduced thickness of E5 and E6, with distortion of small-sized chondrocytes, which had vacuolated cytoplasm (arrow). Diminished staining of the matrix (tailed arrow), empty lacunae (wavy arrow), and areas of the matrix devoid of cells (arrowhead) suggestive of cellular disintegration, and less developed primary ossification centers (C) were seen. Alloxan + arachidonic acid in (c, g, k and o) showed healthy epiphyseal growth plates (E5 and E6) of the vertebrae, with zones of growing chondrocytes, and homogenous distribution of staining in the cartilage matrix. Arachidonic acid group in (d, h, l and p) showed normal histological appearance of the epiphyseal growth plates (E5 and E6). Note the inter-vertebral disk with nucleus pulposus (N) and annulus fibrosus (A). HE staining: (a–d and i–l) ×100, scale bar 100 µm. Masson's trichrome technique: (e–h) ×100, scale bar 100 µm. Toluidine blue staining: (m–p) ×400, scale bar 20 µm. 1: Reserve (R) cells; 2: Proliferative (P) cells; 3: Hypertrophied (H) cells; HE: Hematoxylin–Eosin.***

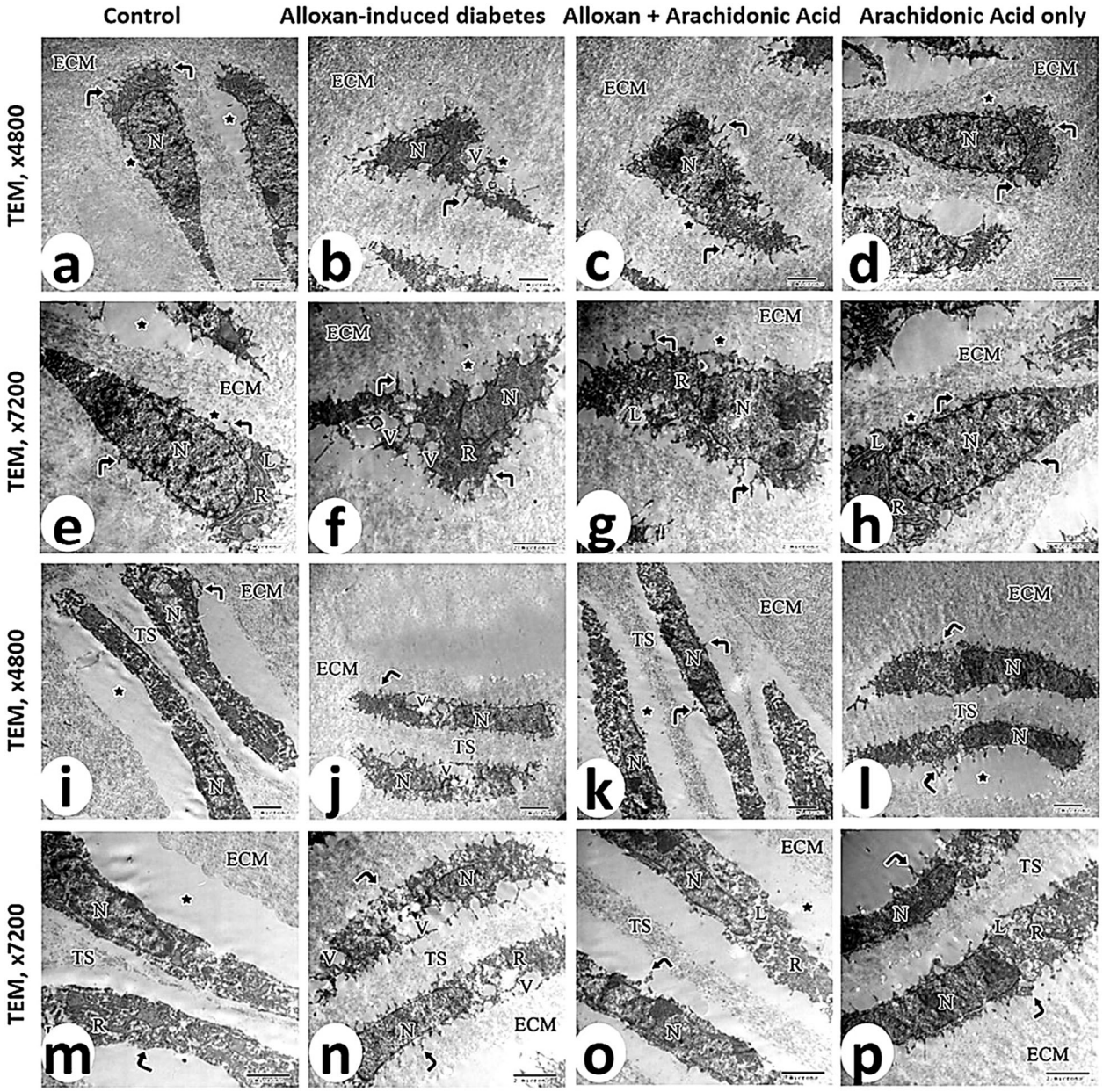

Figure 4 – ***Transmission electron micrographs of ultrathin sections in the three weeks old rats' 6th lumbar vertebrae showing the protective effect of arachidonic acid on alloxan-induced diabetes. Control group showed the ultrastructure of reserve zone cells (a and e) and proliferative zone cells (i and m) of the epiphyseal plates. The reserve cell had triangular shape with large oval nucleus (N) occupying most of the cytoplasm, rough endoplasmic reticulum (R), lipid granules (L), many mitochondria (M), multiple cytoplasmic processes (curved arrows), pericellular space (asterisk), and extracellular matrix (ECM) rich in collagen fibrils. The proliferative cells were flattened and enclosed in lacunae (asterisk), which were separated from each other by transverse septa (TS). The cells showed oval nuclei (N), multiple cytoplasmic processes (curved arrows), lipid granules (L) evident in the cytoplasm, with surrounding ECM rich in collagen fibrils. Alloxan-induced diabetes group in (b, f, j and n) showed shrunken irregular-shaped reserve cells (b and f), with irregular nucleus (N), cytoplasmic vacuolations (V), damaged mitochondria (M); typical of cells undergoing apoptosis, with widened pericellular space (asterisk) and less collagen fibrils in the ECM. The proliferative cells (j and n) were reduced in size with irregular nucleus (N), cytoplasmic vacuolations (V), and less developed rough endoplasmic reticulum (R). Alloxan + arachidonic acid group in (c, g, k and o) showed the cellular structure returned to normal with healthy appearance of the reserve and proliferative cells, which had oval nuclei (N), multiple cytoplasmic processes (curved arrows), many mitochondria (M), preserved pericellular space (asterisk) and ECM rich in collagen fibrils. The proliferative cells were enclosed in lacunae, which were separated from each other by TS. Arachidonic acid group in (d, h, l and p) showed the normal features of reserve and proliferative cells. Uranyl acetate and Lead citrate staining, transmission electron microscopy (TEM): (a–d and i–l) ×4800; (e–h and m–p) ×7200; scale bar 2 µm.***

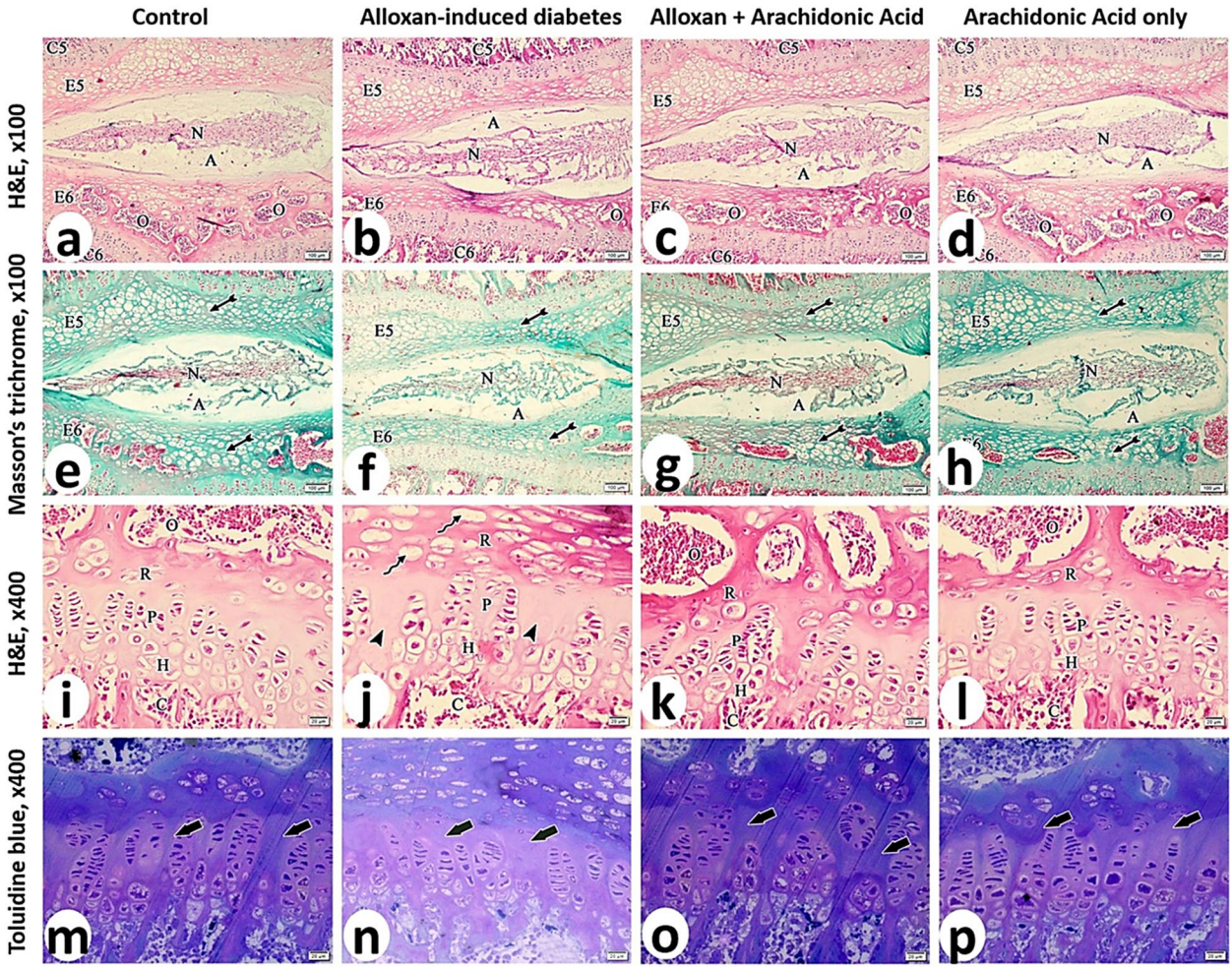

Figure 5 – ***Photomicrographs of the sagittal sections in the two months old rats' 5th and 6th lumbar vertebrae showed the protective effect of arachidonic acid on alloxan-induced diabetes. Control group in (a, e, i and m) showed the epiphyseal growth plates (E5 and E6), with healthy normal appearance of the vertebrae that had zones of growing chondrocytes. The epiphyseal growth plates show normal homogenous distribution of green color (tailed arrow), and Toluidine blue staining in the cartilage matrix (thick arrow) between the growing chondrocytes. Alloxan-induced diabetes group in (b, f, j and n) showed decreased thickness of E5 and E6, with disorganization of growing chondrocytes. Diminished staining of the matrix (tailed arrow), empty lacunae (wavy arrow), and areas of the matrix devoid of cells (arrowhead), and less developed primary (C5 and C6) and secondary ossification (O) centers (C) were seen. Alloxan + arachidonic acid in (c, g, k and o) showed healthy epiphyseal growth plates (E5 and E6) of the vertebrae, with zones of growing chondrocytes, well developed primary (C5 and C6) and secondary ossification (O) centers (C), and homogenous distribution of staining in the cartilage matrix. Arachidonic acid group in (d, h, l and p) showed normal histological appearance of the epiphyseal growth plates (E5 and E6) and ossification (O) centers (C). Note the intervertebral disk with nucleus pulposus (N) and annulus fibrosus (A). HE staining: (a–d and i–l) ×100, scale bar 100 µm. Masson's trichrome technique: (e–h) ×100, scale bar 100 µm. Toluidine blue staining: (m–p) ×400, scale bar 20 µm. H: Hypertrophied cells; HE: Hematoxylin–Eosin; P: Proliferative cells; R: Reserve cells.***

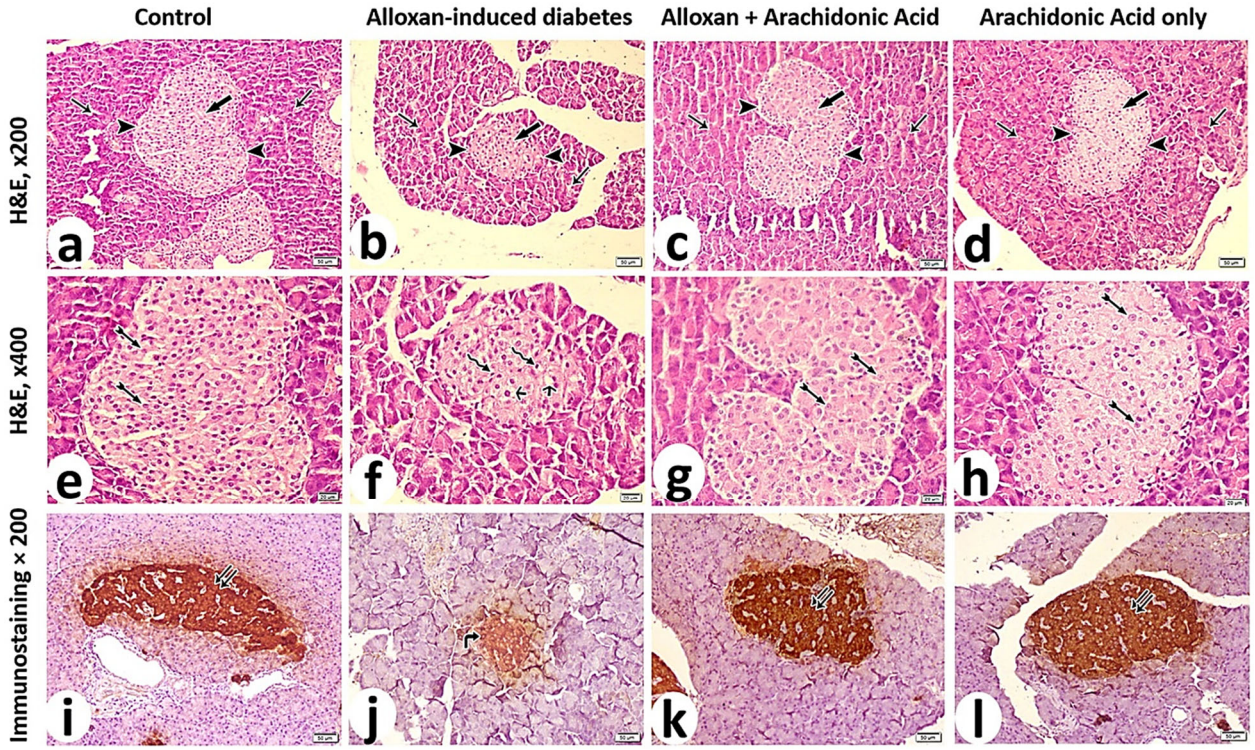

Figure 6 – ***Photomicrographs of paraffin cross-sections in the rats' pancreas of the mothers of the studied groups showed the protective effect of arachidonic acid on alloxan-induced diabetes. Control group in (a, e and i) showed pancreatic islets (thick arrow), which were interspersed between pancreatic acini (arrow), with distinct border (arrowhead), and normal islets cells with vesicular nuclei (tailed arrow). Immunohistochemistry showed localization of β-cells in the islets as intense brown color of insulin immunoexpression (double arrows). Alloxan-induced diabetes group in (b, f and j) showed shrinkage of the pancreatic islets (thick arrow), with faint border between islets and pancreatic acini (arrowhead). Islets cells were atrophied, with apoptotic nuclei (wavy arrow), vacuolations (short arrows), and showed weak insulin immunoexpression (curved arrow). Alloxan + arachidonic acid group in (c, g and k) showed restoration of the healthy features of pancreatic islets, with strong positive insulin immunoreactivity presented as intense brown color (double arrows). Arachidonic acid group in (d, h and l) showed normal appearance of the pancreatic islets, and strong positive insulin immunoreactivity was seen as intense brown color (double arrows). Hematoxylin–Eosin (HE) staining: (a–d) ×200, scale bar 50 µm; (e–h) ×400, scale bar 20 µm. Anti-insulin antibody immunostaining, counterstained with Hematoxylin: (i–l) ×200, scale bar 50 µm.***

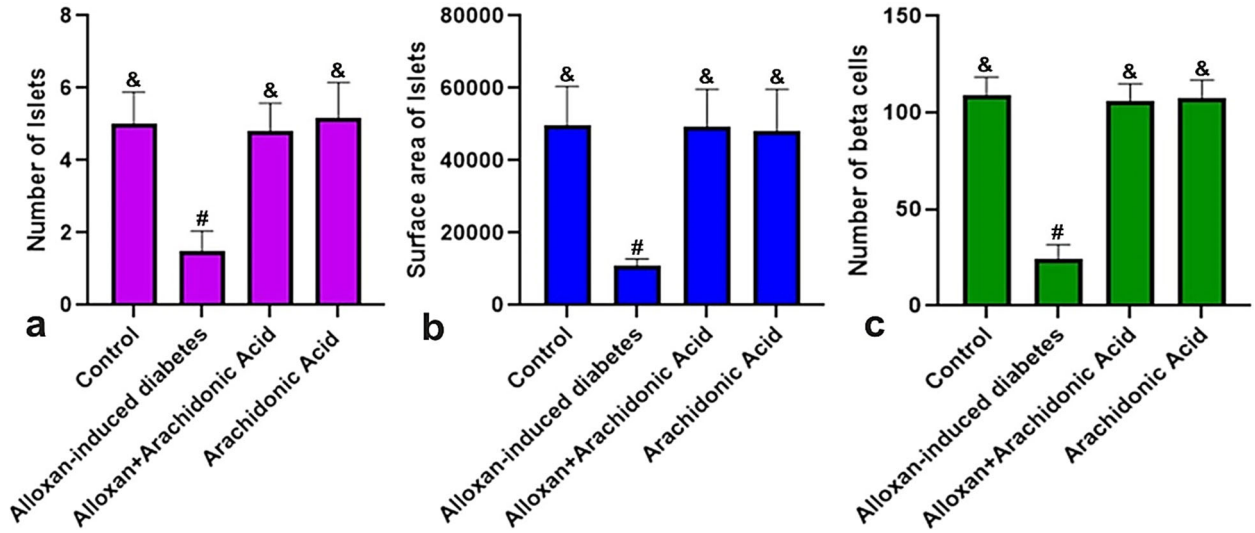

Figure 7 – ***Pancreatic morphometric results of the rats' mothers obtained in the current study analyzed using GraphPad Prism Software version 5 (GraphPad Software Inc., La Jolla, CA, USA): https://www.graphpad.com/scientific-software/prism/. (a) Alloxan significantly decreased the number of pancreatic islets, and the addition of arachidonic acid kept the normal number of islets. (b) Alloxan significantly reduced the surface area of the islets, and the use of arachidonic acid maintained the normal surface area of pancreatic islets. (c) Alloxan significantly decreased the number of β-cells per islet, and the addition of arachidonic acid kept the normal number of β-cells. Results are expressed as the mean ± SD of six rats per group. $^{\&,\#}$Different symbols indicate significant differences at $p<0.05$ (one-way ANOVA followed by Bonferroni's post hoc test). ANOVA: Analysis of variance; SD: Standard deviation.***

Discussions

Diabetes during pregnancy is burdened with a two- to five-fold increase in the risk of birth defects. Even with optimal glycemic control and good pre-gestational care, it has been difficult to normalize the malformation rate [5, 20]. Diabetes in pregnancy increases oxidative stress [21], enhances lipid peroxidation [22, 23], decreases anti-oxidative defense capacity [24], lowers prostaglandin E2 levels, diminishes cyclooxygenase-2 gene expression, and increases apoptosis in the embryo [22]. The disruption of the oxidant/antioxidant balance by high glucose amounts can cause massive cell damage, increase in apoptotic events and defective embryonic development [25]. Infants born to mothers with pre-existing diabetes have increased risk of spine malformations [26], delayed fetal skeletal growth, and retarded ossification [7]. Thus, the searching for chemicals and supplements that have protective effect against diabetic tissue damage is worthwhile. In the current research, arachidonic acid given to diabetic pregnant rats could alleviate the damage of the lumbar vertebrae *via* its cytoprotective properties. Noteworthy, it was reported that in both type 1 and type 2 diabetes mellitus the plasma and tissue arachidonic acid content were low [17]. Arachidonic acid is one of the essential PUFAs that is available in very small amounts in human diet. Earlier studies suggested a potential antidiabetic action for arachidonic acid [17].

In this work, induction of diabetes was carried out by the injection of alloxan. Earlier studies revealed that the diabetic effect of alloxan is mainly attributed to its rapid uptake by the β-cells, increased formation of free radicals and ROS that cause fragmentation of β-cell deoxyribonucleic acid (DNA) and apoptosis, resulting in type 1 diabetes with hyperglycemia and little endogenous insulin production [12, 27]. In this study, gross morphological measurements were recorded as the crown rump length, snout rump length and crown heel length of the newborn, three-week-old, and two-month-old rats. In the alloxan-induced diabetes group, highly significant decrease in all parameters was reported as compared to the control and other groups. Our results were in line with those of previous researchers that revealed growth retardation with decrease in the crown rump length in the embryos of the diabetic rat mothers [25]. The body weights of the newborn, three-week-old, and two-month-old rats were verified in all groups included in this study. In the alloxan-induced diabetes group, significant body weight reductions were found as compared to the control group. These results were concomitant with those of earlier researchers that indicated a lower body weight at birth (microsomia) in the offspring of the diabetic rats, and this decrease in weight remained during the weaning, and juvenile stages [28, 29]. This weight reduction at birth could be due to the high blood glucose amount in the intra-uterine environment during gestational diabetes, resulting in over-stimulation of pancreatic β-cells that prevented insulin secretion, decreasing anabolism and, subsequently, neonatal microsomia [30, 31].

In this study, arachidonic acid disallowed the alloxan-induced diabetes as evident by the normal blood glucose levels in the alloxan + arachidonic acid group. This was in accordance with preceding research that confirmed the role of arachidonic acid in the prevention of both type 1 and type 2 diabetes mellitus [17]. Other investigators added that arachidonic acid not only prevented the development of alloxan-induced diabetes, but also restored the antioxidant status to normalcy [13].

In the present work, the histological findings of the control group showed that the lumbar vertebral body was made of a centrum and two peripheral areas of hyaline cartilage (epiphysis). These results confirmed those of previous researchers that demonstrated the vertebral growth occurring by cartilaginous or endochondral ossification, where mesenchymal cells are transformed into cartilage cells, which subsequently ossify [32]. In this study, the chondrocytes in the epiphyseal growth plates were arranged in four zones: reserve cells, proliferative cells, hypertrophied cells, and calcification zone. In the calcification zone, the hypertrophied chondrocytes were degenerated leaving lacunae, which were invaded by cells from the marrow filled spaces of the centrum. These results supported the previous findings of earlier studies that clarified the structure of the epiphyseal growth plate containing one cell type, the chondrocyte, at different stages of differentiation [33, 34]. Resting zone chondrocytes display a round morphology, and act as the stem-like cells that replenish the pool of proliferative chondrocytes. Proliferative zone chondrocytes acquire a flattened morphology, and at a certain point, they stop dividing and terminally differentiate into hypertrophic chondrocytes. The hypertrophic chondrocytes calcify the surrounding ECM and undergo apoptosis shortly before the blood vessels invade the chondrocyte lacuna [33].

In this study, the morphometrical analysis of the 6th lumbar vertebrae of the newborn, three-week-old, and two-month-old rats in the alloxan-induced diabetes group showed highly significant decrease of the thickness of the epiphyseal growth plate, and less developed primary ossification centers as compared to the control groups. These results were in provision of the highly significant reductions in the crown rump length, snout rump length and crown heel length of the newborn, three-week-old, and two-month-old rats of the alloxan-induced diabetes group in our study. In harmony, another group of researchers showed decrease in thickness of the epiphyseal growth plates of the femur of the diabetic rats [35]. Also, similar results were obtained by other investigators who observed that maternal diabetes delayed the bone ossification in rat fetuses [7, 36]. They also found that the growing chondrocytes were disorganized, distorted, small-sized, and with vacuolated cytoplasm. Furthermore, it has been demonstrated that the violation of the oxidant/antioxidant balance by high glucose levels can cause massive cell damage and increase in apoptotic events [25, 27, 37].

In the control group of this study, Masson's trichrome technique showed intense green color in the matrix due to the abundance of collagen fibers between the growing chondrocytes of epiphyseal plate, and stained deep blue by Toluidine blue staining due to the matrix sulfur in proteoglycans and glycosaminoglycans as reported by earlier studies [38, 39]. In contrast, the alloxan-induced diabetes group of the present study showed markedly diminished staining of the matrix between the growing chondrocytes of the epiphyseal growth plates. These results supported previous studies that reported that hyperglycemia can lead to bone loss, a decrease in bone density, and bone micro-architecture impairment in rats [36, 40]. Also, hyperglycemia

changes the mineral composition and collagen integrity of bones, causing the marrow cavity to become full of fat and adipogenic mesenchymal stem cells [41, 42].

In this study, TEM examination of the reserve and proliferative cells of the alloxan-induced diabetes group of the newborn and three-week-old rats showed shrinkage of the cells, irregular nuclei and cytoplasmic vacuolations. The pericellular spaces and lacunae were widened with sparse collagen fibrils in the ECM as compared with the control group. These findings agreed with other researchers who have found that the hindlimb bones of the embryos of the diabetic mothers exhibited malformed chondrocytes, which possessed vacuolated cytoplasm, massive breakdown of their cytoplasmic compartments, and clumping of their nuclear chromatin indicating apoptosis [36].

In the present study, light microscopy and TEM examination of the lumbar vertebrae of the alloxan + arachidonic acid group of the newborn, three-week-old, and two-month-old rats showed normal tissue and cell structure. Arachidonic acid provided cytoprotection against the development of alloxan-induced apoptosis, which can be explained based on the antidiabetic properties of arachidonic acid [17]. Based on our findings, the mothers of this group showed normal blood glucose level, so these results confirmed the role of arachidonic acid in prevention of alloxan-induced diabetes. These findings supported those of other scientists who illustrated that arachidonic acid prevents the apoptotic action of alloxan as it prevents DNA fragmentation protecting the integrity of the β-cells and thus, the cells retain their functional capacity [43]. This is an important aspect for β-cells since, its ability to secrete insulin is important to prevent diabetes and control hyperglycemia.

To find a possible explanation of the modulatory mechanism through which arachidonic acid would exert its antidiabetic protective effect, we extended our research to assess the pancreatic structure and insulin expression in the studied groups. In this work, light microscopy of the pancreas of rats' mothers of alloxan-induced diabetes group showed marked shrinkage of the pancreatic islets, and the islet cells appeared atrophied with apoptotic nuclei, as compared to the control group. Similar results were observed by researchers who revealed pathological changes of endocrine part of the pancreas with marked degeneration and necrosis of β-cells, which showed pyknotic nuclei and vacuolations [44, 45]. In addition, previous research studies highlighted that alloxan induces a diabetes-like state in animals as it is taken up by β-cells, and its reduction by hexokinase induces a redox cycle that increases the production of ROS and leads to β-cell necrosis [12]. In this study, light microscopy of the pancreas in the rats' mothers of the alloxan + arachidonic acid group showed remarkable improvement in the histoarchitecture simulating the control group. This could be attributed to the anti-diabetic action of arachidonic acid [17].

In our research, the immunohistochemistry of the pancreas of the rats' mothers of the studied groups revealed insulin expression in the pancreatic islets. In alloxan-induced diabetes group, very weak insulin immunoreactivity was detected in the cytoplasm of β-cells of shrunken pancreatic islets. These findings agreed with previous studies that detected decreased insulin immunoreactivity in the pancreatic islets of their alloxan-induced diabetes group [44, 46]. In this work, in the rats' mothers of the alloxan + arachidonic acid group, insulin showed strong positive immunoexpression within the β-cells of pancreatic islets. These findings were in harmony with other researchers who revealed that arachidonic acid prevented alloxan-induced diabetes and restored the antioxidant status to normalcy [13, 17].

In this study, the morphometrical analysis included the number of pancreatic islets, surface area of the islets, and the number of β-cells per islet in the rats' mothers of this research groups. In alloxan-induced diabetes group, highly significant decrease in all parameters was found as compared to the control group. These results supported those of other scientists who detected massive destruction of insulin secreting β-cells of islets of Langerhans in diabetic rats, including decreased islets cell numbers, and increased cell death in the pancreas [47]. In alloxan + arachidonic acid group and arachidonic acid group, there were no significant differences in the number of pancreatic islets, surface area of the islets, and the number of β-cells per islet as compared to the control. This outcome may be attributed to the anti-diabetic action of arachidonic acid [17].

Conclusions

This study illustrated the protective effect of arachidonic acid against structural and ultrastructural bony deteriorations associated with alloxan-induced diabetes through restoring the lumbar vertebrae structure and insulin immunoexpression in the pancreatic β-cells and exerting anti-apoptotic effect. This research needs to be repeated on several experimental animals before testing it on human volunteers. Based on our results, it is suggested to recommend giving arachidonic acid to diabetics who have bone problems. However, future research is needed to decide on the safe dose and duration of arachidonic acid intake for diabetic pregnant women. Moreover, the results of this study are of outmost significance in paving the road towards incorporation of arachidonic acid in our food industry as prophylaxis against diabetes, and to fight against the diabetes-associated abnormalities.

Conflict of interests

The authors declare that there is no conflict of interests.

Compliance with Ethical Statements

All applicable international, national, and/or institutional guidelines for the care and use of animals were followed.

Ethical Approval

This experimental research protocol was approved by the Local Ethics Committee and by the Institutional Review Board of Faculty of Medicine, Assiut University (Approval No. 17200437 on May 07, 2020).

Funding

This research did not receive any funding/grant from funding agencies in the public, commercial, or not-for-profit sectors.

Authors' contribution

Refaat Shehata Mohamed, Ayman Salaheldeen Amer, Ashraf Edward Bastwrous and Martha Emil Adly designed the research; Martha Emil Adly acquired the data. Ayman Salaheldeen Amer and Martha Emil Adly recorded the measurements. Ayman Salaheldeen Amer and Martha Emil

Adly analyzed the data and wrote the manuscript. All authors discussed the results and commented on the manuscript.

All data generated or analyzed during this study are included in this article. Further enquiries can be directed to the corresponding author.

References

[1] Bell R, Bailey K, Cresswell T, Hawthorne G, Critchley J, Lewis-Barned N; Northern Diabetic Pregnancy Survey Steering Group. Trends in prevalence and outcomes of pregnancy in women with pre-existing type I and type II diabetes. BJOG, 2008, 115(4):445–452. https://doi.org/10.1111/j.1471-0528.2007.01644.x PMID: 18271881

[2] Eriksson UJ, Wentzel P. The status of diabetic embryopathy. Ups J Med Sci, 2016, 121(2):96–112. https://doi.org/10.3109/03009734.2016.1165317 PMID: 27117607 PMCID: PMC4900070

[3] Dabelea D, Mayer-Davis EJ, Lamichhane AP, D'Agostino RB Jr, Liese AD, Vehik KS, Narayan KMV, Zeitler P, Hamman RF. Association of intrauterine exposure to maternal diabetes and obesity with type 2 diabetes in youth: the SEARCH case–control study. Diabetes Care, 2008, 31(7):1422–1426. https://doi.org/10.2337/dc07-2417 PMID: 18375420 PMCID: PMC2453655

[4] Knight KM, Pressman EK, Hackney DN, Thornburg LL. Perinatal outcomes in type 2 diabetic patients compared with non-diabetic patients matched by body mass index. J Matern Fetal Neonatal Med, 2012, 25(6):611–615. https://doi.org/10.3109/14767058.2011.587059 PMID: 21728737

[5] Vinceti M, Malagoli C, Rothman KJ, Rodolfi R, Astolfi G, Calzolari E, Puccini A, Bertolotti M, Lunt M, Paterlini L, Martini M, Nicolini F. Risk of birth defects associated with maternal pregestational diabetes. Eur J Epidemiol, 2014, 29(6):411–418. https://doi.org/10.1007/s10654-014-9913-4 PMID: 24861339

[6] Zhao J, Weiler HA. Long-term effects of gestational diabetes on offspring health are more pronounced in skeletal growth than body composition and glucose tolerance. Br J Nutr, 2010, 104(11):1641–1649. https://doi.org/10.1017/S0007114510002631 PMID: 20615268

[7] Sirasanagandla SR, Ranganath Pai KS, Potu BK, Bhat KM. Protective effect of *Cissus quadrangularis* Linn. on diabetes induced delayed fetal skeletal ossification. J Ayurveda Integr Med, 2014, 5(1):25–32. https://doi.org/10.4103/0975-9476.128852 PMID: 24812472 PMCID: PMC4012358

[8] Shamsi MM, Ranjbar R, Khaksary Mahabady M, Tabandeh MR, Khazaeel K, Najafzadeh H. Protective effect of quercetin on morphological and histometrical changes of placenta in streptozotocin-induced diabetic rat. Zahedan J Res Med Sci, 2020, 22(1):e88636. https://doi.org/10.5812/zjrms.88636 https://sites.kowsarpub.com/zjrms/articles/88636.html

[9] Xian CJ, Howarth GS, Cool JC, Foster BK. Effects of acute 5-Fluorouracil chemotherapy and insulin-like growth factor-I pretreatment on growth plate cartilage and metaphyseal bone in rats. Bone, 2004, 35(3):739–749. https://doi.org/10.1016/j.bone.2004.04.027 PMID: 15336611

[10] Yilmaz S, Tokpinar A. Double staining in rats (mini review). Biomed J Sci Tech Res, 2019, 16(4):12282–12285. https://doi.org/10.26717/BJSTR.2019.16.002899 https://biomedres.us/fulltexts/BJSTR.MS.ID.002899.php

[11] Nilsson O, Marino R, De Luca F, Phillip M, Baron J. Endocrine regulation of the growth plate. Horm Res, 2005, 64(4):157–165. https://doi.org/10.1159/000088791 PMID: 16205094

[12] Szkudelski T. The mechanism of alloxan and streptozotocin action in B cells of the rat pancreas. Physiol Res, 2001, 50(6):537–546. PMID: 11829314

[13] Suresh Y, Das UN. Protective action of arachidonic acid against alloxan-induced cytotoxicity and diabetes mellitus. Prostaglandins Leukot Essent Fatty Acids, 2001, 64(1):37–52. https://doi.org/10.1054/plef.2000.0236 PMID: 11161584

[14] Gundala NKV, Naidu VGM, Das UN. Amelioration of streptozotocin-induced type 2 diabetes mellitus in Wistar rats by arachidonic acid. Biochem Biophys Res Commun, 2018, 496(1):105–113. https://doi.org/10.1016/j.bbrc.2018.01.007 PMID: 29309791

[15] Dixon G, Nolan J, McClenaghan NH, Flatt PR, Newsholme P. Arachidonic acid, palmitic acid and glucose are important for the modulation of clonal pancreatic beta-cell insulin secretion, growth and functional integrity. Clin Sci (Lond), 2004, 106(2):191–199. https://doi.org/10.1042/CS20030261 PMID: 14561212

[16] Confavreux CB, Levine RL, Karsenty G. A paradigm of integrative physiology, the crosstalk between bone and energy metabolisms. Mol Cell Endocrinol, 2009, 310(1–2):21–29. https://doi.org/10.1016/j.mce.2009.04.004 PMID: 19376193 PMCID: PMC3667507

[17] Das UN. Arachidonic acid in health and disease with focus on hypertension and diabetes mellitus: a review. J Adv Res, 2018, 11:43–55. https://doi.org/10.1016/j.jare.2018.01.002 PMID: 30034875 PMCID: PMC6052660

[18] Saleh MNM, Hassan SAS, Mahmoud FY, Shenouda MBK. The effect of maternal-induced diabetes on postnatal development of the paraventricular and ventromedial hypothalamic nuclei in albino rats: a histological, immunohistochemical, and morphometric study. J Curr Med Res Pract, 2017, 2(1):47–62. https://doi.org/10.4103/JCMRP.JCMRP_34_16 http://www.jcmrp.eg.net/text.asp?2017/2/1/47/210308

[19] Goto S, Morigaki R, Okita S, Nagahiro S, Kaji R. Development of a highly sensitive immunohistochemical method to detect neurochemical molecules in formalin-fixed and paraffin-embedded tissues from autopsied human brains. Front Neuroanat, 2015, 9:22. https://doi.org/10.3389/fnana.2015.00022 PMID: 25784860 PMCID: PMC4347496

[20] Eidem I, Stene LC, Henriksen T, Hanssen KF, Vangen S, Vollset SE, Joner G. Congenital anomalies in newborns of women with type 1 diabetes: nationwide population-based study in Norway, 1999–2004. Acta Obstet Gynecol Scand, 2010, 89(11):1403–1411. https://doi.org/10.3109/00016349.2010.518594 PMID: 20929418

[21] Yang X, Borg LA, Eriksson UJ. Altered metabolism and superoxide generation in neural tissue of rat embryos exposed to high glucose. Am J Physiol, 1997, 272(1 Pt 1):E173–E180. https://doi.org/10.1152/ajpendo.1997.272.1.E173 PMID: 9038867

[22] Wentzel P, Welsh N, Eriksson UJ. Developmental damage, increased lipid peroxidation, diminished cyclooxygenase-2 gene expression, and lowered prostaglandin E2 levels in rat embryos exposed to a diabetic environment. Diabetes, 1999, 48(4):813–820. https://doi.org/10.2337/diabetes.48.4.813 PMID: 10102698

[23] Cederberg J, Basu S, Eriksson UJ. Increased rate of lipid peroxidation and protein carbonylation in experimental diabetic pregnancy. Diabetologia, 2001, 44(6):766–774. https://doi.org/10.1007/s001250051686 PMID: 11440370

[24] Ornoy A, Zaken V, Kohen R. Role of reactive oxygen species (ROS) in the diabetes-induced anomalies in rat embryos *in vitro*: reduction in antioxidant enzymes and low-molecular-weight antioxidants (LMWA) may be the causative factor for increased anomalies. Teratology, 1999, 60(6):376–386. https://doi.org/10.1002/(SICI)1096-9926(199912)60:6<376::AID-TERA10>3.0.CO;2-Q PMID: 10590399

[25] Zangen SW, Yaffe P, Shechtman S, Zangen DH, Ornoy A. The role of reactive oxygen species in diabetes-induced anomalies in embryos of Cohen diabetic rats. Int J Exp Diabetes Res, 2002, 3(4):247–255. https://doi.org/10.1080/15604280214933 PMID: 12546278 PMCID: PMC2478588

[26] Aberg A, Westbom L, Källén B. Congenital malformations among infants whose mothers had gestational diabetes or preexisting diabetes. Early Hum Dev, 2001, 61(2):85–95. https://doi.org/10.1016/s0378-3782(00)00125-0 PMID: 11223271

[27] King AJ. The use of animal models in diabetes research. Br J Pharmacol, 2012, 166(3):877–894. https://doi.org/10.1111/j.1476-5381.2012.01911.x PMID: 22352879 PMCID: PMC3417415

[28] Piazza FV, Segabinazi E, de Meireles ALF, Mega F, Spindler CF, Augustin OA, Salvalaggio GDS, Achaval M, Kruse MS, Coirini H, Marcuzzo S. Severe uncontrolled maternal hyperglycemia induces microsomia and neurodevelopment delay accompanied by apoptosis, cellular survival, and neuroinflammatory deregulation in rat offspring hippocampus. Cell Mol Neurobiol, 2019, 39(3):401–414. https://doi.org/10.1007/s10571-019-00658-8 PMID: 30739252

[29] Huerta-Cervantes M, Peña-Montes DJ, Montoya-Pérez R, Trujillo X, Huerta M, López-Vázquez MA, Olvera-Cortés ME,

Saavedra-Molina A. Gestational diabetes triggers oxidative stress in hippocampus and cerebral cortex and cognitive behavior modifications in rat offspring: age- and sex-dependent effects. Nutrients, 2020, 12(2):376. https://doi.org/10.3390/nu12020376 PMID: 32023917 PMCID: PMC7071266

[30] Aerts L, Van Assche FA. Animal evidence for the transgenerational development of diabetes mellitus. Int J Biochem Cell Biol, 2006, 38(5–6):894–903. https://doi.org/10.1016/j.biocel.2005.07.006 PMID: 16118061

[31] Fetita LS, Sobngwi E, Serradas P, Calvo F, Gautier JF. Consequences of fetal exposure to maternal diabetes in offspring. J Clin Endocrinol Metab, 2006, 91(10):3718–3724. https://doi.org/10.1210/jc.2006-0624 PMID: 16849402

[32] DeSesso JM, Scialli AR. Bone development in laboratory mammals used in developmental toxicity studies. Birth Defects Res, 2018, 110(15):1157–1187. https://doi.org/10.1002/bdr2.1350 PMID: 29921029

[33] Mackie EJ, Tatarczuch L, Mirams M. The skeleton: a multifunctional complex organ: the growth plate chondrocyte and endochondral ossification. J Endocrinol, 2011, 211(2):109–121. https://doi.org/10.1530/JOE-11-0048 PMID: 21642379

[34] Guevara-Morales JM, Frohbergh M, Castro-Abril H, Vaca-González JJ, Barrera LA, Garzón-Alvarado DA, Schuchman E, Simonaro C. Growth plate pathology in the mucopolysaccharidosis type VI rat model – an experimental and computational approach. Diagnostics (Basel), 2020, 10(6):360. https://doi.org/10.3390/diagnostics10060360 PMID: 32486376 PMCID: PMC7344727

[35] Ma R, Wang L, Zhao B, Liu C, Liu H, Zhu R, Chen B, Li L, Zhao D, Mo F, Li Y, Niu J, Jiang G, Fu M, Bromme D, Gao S, Zhang D. Diabetes perturbs bone microarchitecture and bone strength through regulation of Sema3A/IGF-1/β-catenin in rats. Cell Physiol Biochem, 2017, 41:55–66. https://doi.org/10.1159/000455936 PMID: 28135705

[36] El-Sayyad HIH, El-Ghawet HA, Al-Haggar MS, Bakr IH. Impairment of bone growth of Wistar rat fetuses of diabetic and hypercholesterolemic mothers. Egypt J Basic Appl Sci, 2015, 2(1):1–12. https://doi.org/10.1016/j.ejbas.2014.12.003 https://www.tandfonline.com/doi/full/10.1016/j.ejbas.2014.12.003

[37] Eriksson JG, Ylihärsilä H, Forsén T, Osmond C, Barker DJP. Exercise protects against glucose intolerance in individuals with a small body size at birth. Prev Med, 2004, 39(1):164–167. https://doi.org/10.1016/j.ypmed.2004.01.035 PMID: 15207998

[38] Schmitz N, Laverty S, Kraus VB, Aigner T. Basic methods in histopathology of joint tissues. Osteoarthritis Cartilage, 2010, 18(Suppl 3):S113–S116. https://doi.org/10.1016/j.joca.2010.05.026 PMID: 20864017

[39] Obeid RF, Abdelmoneim HS, Elsharkawy RT. Histological evaluation of the antioxidant effect of vitamin E on reversing the negative impact of Tartrazine on extraction socket healing (randomized controlled trial). Egypt Dent J, 2020, 66(1):285–292. https://doi.org/10.21608/EDJ.2020.77544 https://edj.journals.ekb.eg/article_77544.html

[40] Shanbhogue VV, Hansen S, Frost M, Jørgensen NR, Hermann AP, Henriksen JE, Brixen K. Bone geometry, volumetric density, microarchitecture, and estimated bone strength assessed by HR-pQCT in adult patients with type 1 diabetes mellitus. J Bone Miner Res, 2015, 30(12):2188–2199. https://doi.org/10.1002/jbmr.2573 PMID: 26096924

[41] McCarthy AD, Uemura T, Etcheverry SB, Cortizo AM. Advanced glycation endproducts interfere with integrin-mediated osteoblastic attachment to a type-I collagen matrix. Int J Biochem Cell Biol, 2004, 36(5):840–848. https://doi.org/10.1016/j.biocel.2003.09.006 PMID: 15006636

[42] Kume S, Kato S, Yamagishi S, Inagaki Y, Ueda S, Arima N, Okawa T, Kojiro M, Nagata K. Advanced glycation end-products attenuate human mesenchymal stem cells and prevent cognate differentiation into adipose tissue, cartilage, and bone. J Bone Miner Res, 2005, 20(9):1647–1658. https://doi.org/10.1359/JBMR.050514 PMID: 16059636

[43] Gundala NKV, Naidu VGM, Das UN. Arachidonic acid and lipoxin A4 attenuate alloxan-induced cytotoxicity to RIN5F cells *in vitro* and type 1 diabetes mellitus *in vivo*. BioFactors, 2017, 43(2):251–271. https://doi.org/10.1002/biof.1336 PMID: 27862450

[44] Abdul-Hamid M, Moustafa N. Protective effect of curcumin on histopathology and ultrastructure of pancreas in the alloxan treated rats for induction of diabetes. J Basic Appl Zool, 2013, 66(4):169–179. https://doi.org/10.1016/j.jobaz.2013.07.003 https://www.sciencedirect.com/science/article/pii/S2090989613000234

[45] Rajesh R, Sreekala V. Characterisation of streptozotocin induced diabetes mellitus in Wistar albino rats – a histological and haematological perspective. MedPulse Int J Anat, 2020, 13(2):33–36. https://doi.org/10.26611/10011323 https://medpulse.in/Anatomy/html_13_2_3.php

[46] Simsek N, Kaya M, Kara A, Can I, Karadeniz A, Kalkan Y. Effects of melatonin on islet neogenesis and beta cell apoptosis in streptozotocin-induced diabetic rats: an immunohistochemical study. Domest Anim Endocrinol, 2012, 43(1):47–57. https://doi.org/10.1016/j.domaniend.2012.02.002 PMID: 22541933

[47] Balaji P, Madhanraj R, Rameshkumar K, Veeramanikandan V, Eyini M, Arun A, Thulasinathan B, Al Farraj DA, Elshikh MS, Alokda AM, Mahmoud AH, Tack JC, Kim HJ. Evaluation of antidiabetic activity of *Pleurotus pulmonarius* against streptozotocin–nicotinamide induced diabetic Wistar albino rats. Saudi J Biol Sci, 2020, 27(3):913–924. https://doi.org/10.1016/j.sjbs.2020.01.027 PMID: 32127771 PMCID: PMC7042672

Corresponding author

Ayman Salaheldeen Amer, Professor, PhD, Department of Human Anatomy and Embryology, Faculty of Medicine, Assiut University, 71526 Assiut, Egypt; Phone 00201061461342, Fax 0020882332278, e-mail: ayman.amer@aun.edu.eg

Received: August 30, 2021

Accepted: August 8, 2022